Climate Dynamics (2005) 24: 793–807
DOI 10.1007/s00382-004-0488-8

A. M. Duan · G. X. Wu

Role of the Tibetan Plateau thermal forcing in the summer climate patterns over subtropical Asia

Received: 27 May 2004 / Accepted: 20 October 2004 / Published online: 13 May 2005

Abstract The mechanism of the Tibetan Plateau (TP) thermal forcing in influencing the summer climate patterns over subtropical Asia is investigated by means of NCEP/NCAR reanalysis diagnosis. Results show that since the TP is a huge elevated heating source with the strongest heating in the surface layers in summer, the thermal adaptation results in a shallow cyclonic circulation near the surface and a deep anticyclonic circulation above it. According to the steady barotropic vorticity equation for large scales, airflow must converge in the lower layers and diverge in the higher layers over the eastern side of the TP. However, the western side of the TP is characterized by a reversed structure, i.e., divergence in lower layers but convergence in higher layers. Hence, pumping and sucking processes bring in upward and downward movement over the east and west sides of the TP, respectively. Such a circulation is embedded in the large-scale circulation that is forced by the Eurasian continental heating. Because the TP together with Iran Plateau are located at the central and eastern parts of the continent, and, because the orography-induced circulation is in phase with the continental scale circulation, the role of the TP thermal forcing is to intensify the East Asian monsoon to its east and the dry and hot desert climate in mid-Asia to its west. The summertime thermal forcing of the Rockies and Andes can generate similar circulations along the two subtopics as the TP does since they are located near the western coasts. But, the lower troposphere poleward flow that is induced by orographic thermal forcing does not coincide with the poleward flows over the eastern coastal region that is induced by continental heating and the monsoon rainfall in North and South America is not as strong as in East Asia. However, the equatorward flow and the associated subsidence induced by the two mountain ranges along the western coasts of both North and South America are in phase with those induced by continental heating. These contribute to the formation of the stable low stratus clouds and strong long-wave radiative cooling over the eastern subtropical Pacific regions just off the western coast of the continent.

A. M. Duan · G. X. Wu (✉)
State Key Laboratory of Numerical Modeling for Atmospheric Sciences and Geophysical Fluid Dynamics (LASG),
Institute of Atmospheric Physics (IAP),
Chinese Academy of Sciences (CAS),
Beijing, 100029, China
E-mail: gxwu@lasg.iap.ac.cn

1 Introduction

It is well known that a large-scale mountain exerts significant influence on the atmospheric circulation through its mechanical and thermodynamical effects. Pioneering observation diagnoses such as Yin (1949), Yeh (1950), Flohn (1957), Yeh et al. (1957), Murakami (1958), Koteswaram (1958), and Staff Members of Academia Sinica (1957) have revealed the features of circulation and heating in different seasons over the Tibetan Plateau (TP) and discussed their possible connection with the mechanical and thermal aspects of the TP forcing. These papers, accompanied by theoretical and numerical modeling studies (e.g., see Charney and Eliassen 1949; Bolin 1950; Hoskins and Karoly 1981; Wu 1984; Rodwell and Hoskins 2001) have revealed the important role of mechanical forcing in the formation of atmospheric circulation in winter. However, the circulation in the summer subtropics seems to be more related to thermal forcing, and its formation mechanism is more complicated compared to other latitudes (Hoskins 1987; Rodwell and Hoskins 2001) . According to the results of numerical simulation and data analysis, Rodwell and Hoskins (2001) argued that the subtropical circulation in summer comprises a set of weakly interacting monsoon systems, each involving monsoon rains, a low-level poleward jet, a subtropical anticyclone to the east, and descent and equatorward flow to the west. A local "diabatic enhancement", which is produced by interaction

of the Rossby wave and the midlatitude westerlies, can lead to a strengthening of the descent. Nevertheless, the onset of the Asian summer monsoon is closely linked to the thermal and mechanical forcing of the TP, and only under the condition of the existence of the TP, can the monsoon climate extend northward to the real situation (Yin 1949; Hahn and Manabe 1975; Wu and Zhang 1998).

In addition to mechanical forcing, some earlier theoretical researches have also indicated that planetary scale phenomena can be excited or maintained by thermal forcing alone (Smagorinsky 1953, Döös 1962, Gill 1980). Recently, a quadruple heating pattern (Wu and Liu 2003; Liu et al. 2004) has been found over each subtropical continent and its adjacent oceans in summer. The ocean region to the west is characterized by strong long-wave radiative cooling (LO); the western and eastern portions of the continent are dominated by sensible heating (SE) and condensation heating (CO), respectively; and the ocean region to the east is characterized by double dominant heating (D), with LO prevailing CO. These compose a LO-SE-CO-D heating quadruplet. Its general feature is heating over the continent and cooling over the oceans. A distinct circulation pattern accompanies this heating pattern: in the upper troposphere, anticyclonic circulations over the continent is accompanied by cyclonic circulation over the oceans on its western and eastern sides; near the surface, cyclonic circulation over the continent is accompanied by anticyclonic circulations over the oceans on both sides. This circulation feature can be interpreted as the atmospheric thermal adaptation to the continental-scale quadruplet heating. However, the thermal and mechanical impacts of large-scale terrains have not been taken into account in their work.

As a huge, intense, and elevated heat source with strong sensible heating in the surface layers in summer, the TP is located at the subtropical central and eastern Eurasian Continent. Previous studies have shown that its thermal forcing plays a role not only in the formation of summer circulation (Yeh et al. 1957; Flohn 1957, 1960, Yanai et al. 1992; Li and Yanai 1996; Li WP et al. 2001; Zhao and Chen 2001), but also in the development of weather systems over East China (Tao and Ding 1981) and the boreal climate patterns (Hahn and Manabe 1975; Broccoli and Manabe 1992). However, the interaction of the heating effect of the TP with that of the aforementioned continental-scale heating in influencing the circulation and climate pattern is far from clear.

The present effort is an attempt to demonstrate the mechanism of the TP thermal forcing in forming the summer climate patterns over subtropical Asia in contrast to the continental heating. The structure of this paper is as follows. The quality of the NCEP/NCAR reanalysis data used in this study is discussed in the following section. In Sec. 3, the summertime spatial distribution and vertical structure of individual and total diabatic heating over the TP and the neighboring regions are investigated. In Sec. 4, we briefly outline the corresponding circulation and vertical velocity field over subtropical Asia. Section 5 is devoted to giving a sketch diagram of the mechanism of the TP thermal forcing in the summer climate patterns over subtropical Asia. Then the similar summertime circulation patterns over the two other subtropical large-scale mountains, i.e., the Rocky and Andes Mountains, are compared with the TP in Sec. 6. Conclusions and discussions are presented in Sec. 7.

2 Quality of the NCEP/NCAR reanalysis over subtropical Asia

The heating rate, wind speed, vertical velocity, and air temperature fields used in this study are from the monthly mean NCEP/NCAR reanalysis (Kalnay et al. 1996) from 1980 to 1999. The heating rate and precipitation rate is provided at 28 σ levels in the vertical with a 1.875°×1.875° horizontal resolution, and 2.5°×2.5° for other variables. Sensible heating (SH) comes from the integral of vertical diffusive heating and equals to the SH flux. In this work, the total atmospheric diabatic heating or the heat source/sink for a given air column is defined as the sum of the vertical integrals of vertical diffusion, large-scale condensation, deep convection, shallow convection, long-wave radiation, and short-wave radiation heating. In view of the orographic complexity in East Asia, some p - coordinate fields are interpolated to σ - coordinates so that the comparison over different terrains can be more convenient. Since data provided by a GCM, such as the NCEP/NCAR data, have an overall intrinsic limit of reliability in areas with complex orography, it is necessary to test the quality of the NCEP/NCAR reanalysis data over the TP and the nearby regions before performing our analysis in this work.

Generally, NCEP/NCAR reanalysis is considered inferior to the ECMWF reanalysis (ERA) in moisture in the tropics and monsoon region. This has been documented by Trenberth and Guillent (1998), Yanai and Tomita (1998) and more thoroughly by Annamalai et al. (1999). The "heating components" and their vertical profiles of the NCEP/NCAR reanalysis are model-dependent. The condensation heating consists of heating due to stratiform rain and cumulus-induced rain, and the latter is obviously dependent on the cumulus parameterization scheme. The surface SH flux is determined by the temperature difference between land and air and the surface wind and more strongly depends on model. It possesses special features over the TP in observation as reported by Yanai et al. (1973, 1992), Yeh and Gao (1979), Luo and Yanai (1984), Yanai and Li (1994), and Ueda et al. (2003). Caution is then required when the model generated SH is used. Here, we first investigate the surface SH flux of NCEP/NCAR by comparing its values at adjacent grid points with those calculated by Li et al. (2000, 2001) at six automatic meteorology stations (AMS) installed at Lhasa, Rikeze, Lingzi, Nagqu, Gaize, and Shiquanhe as indicated in

Fig. 2b by the triangles. These AMS stations were placed under the Experiment of Surface Energy and Moisture Cycle over the TP from 1995 to 1999. The detailed geographical information of the stations is given in Table 1. The comparisons are shown in Fig.1. Similar results from ECMWF reanalysis are also presented in the figure for comparison. Clearly, the SH temporal variations of the NCEP/NCAR-, ECMWF-, and AMS-based results behave similarly on the monthly mean scale at all six stations, and the correlation coefficients between NCEP/NCAR and AMS (upper right corner in each panel) at Lhasa and Rikeze are 0.69 and 0.76 respectively, passing the significance test level of 0.001. The obvious disagreement at Lingzi may result from very complicated topography in the valley of Brahmaputra. From April to September, the surface SH flux at Gaize and Shiquanhe (western Tibet) remains above 60 W m^{-2}, whereas, those at the other four stations (mid and eastern Tibet) oscillate greatly. This is consistent with the early results (Yeh and Gao 1979; Zhao and Chen 2001) and reflects the scarcity of rainfall over the western TP. An obvious discrepancy is that except at Rikeze, the model-produced surface SH flux in either NCEP/NCAR or ECMWF is always weaker than that based on AMS. This may lead to an underestimation of the importance of SH in the total diabatic heating over the TP by using the reanalysis. It is necessary to point out that due to the differences in spatial resolution (ECMWF on a 2.5°×2.5° grid mesh) and in grid/station elevation, we can not infer which of them is better, even though the correlation coefficient between NCEP/NCAR- and AMS-based (r_{12}) is always larger than that between ECMWF- and AMS-based (r_{13}). Despite this, the similarity in temporal and spatial variations of the two reanalysis data sets and the observations is encouraging, since the goal in this study is to investigate the large-area and long-term mean diabatic heating and the corresponding circulation patterns, these discrepancies will not affect the following qualitative study very much.

Latent heating (LH) is induced by precipitation, thereby the reliability of LH in the NCEP/NCAR reanalysis can be examined by checking the associated precipitation field. Figure 2a and b present the July mean precipitation fields of the NCEP/NCAR and Xie-Arkin data (Xie and Arkin 1996, 1998), which is heavily based on satellite observation when rain gauge data are not sufficient, in the period from 1978 to 1998. It is evident that there are remarkable differences in East Asia. For example, the precipitation centers located on the western side of the TP (69°E, 32°N), the southwestern side of the TP (88°E, 27°N), and the southeastern TP (102°E, 30°N) in NCEP/NCAR cannot be found in Xie-Arkin's, and the magnitude in South and East China in NCEP/NCAR is about 4 mm per day larger than that of Xie-Arkin. Owing to scarce observational stations in the remote sites of the TP, it is inappropriate to draw a conclusion about the quality of NCEP/NCAR precipitation data in the region. However, as shown in Fig. 2, the rainfall rate over the TP region in NCEP/NCAR is about double that in Xie and Arkin. Therefore, the LH over the TP in NCEP/NCAR is to some extent exaggerated. This is in agreement with the diagnosis of Trenberth and Guillemot (1999) . Despite all these discrepancies, the general distribution of these two datasets, which is represented by the decreasing rainfall from the southeast to northwest TP, is basically the same (in particular, the center with more than 14 mm of rainfall per day exists over the northern Bay of Bengal). Furthermore, the vertical distributions of LH at different sites as deduced from the water budget equation (Q_2) and NCEP/NCAR reanalysis are quite similar to those from observations as reported by Yanai and Tomita (1998). Therefore, the NCEP/NCAR LH data are used for the present qualitative study with caution.

As for the upper-level data such as geopotential height, air temperature and horizontal wind fields, the first author (Duan 2003) has compared both the temporal variation and spatial structure between the NCEP/NCAR and another reanalysis dataset GEWEX Asian Monsoon Experiment Intensified Observation Period (GAME-IOP, refers to Matsumoto et al. 1999) with the same horizontal resolution and vertical levels from April to October 1998. The results showed that on the monthly mean time-scale and a spatial resolution of 2.5°×2.5°, the discrepancy between them is insignificant.

3 Features of the summertime diabatic heating over the TP and its neighborhood

Figure 3 presents the climate mean annual cycle of the total diabatic heating and its components averaged over the TP area (75°–105°E, 27.5°–37.5°N). The total diabatic heating increases with the seasonal evolution from

Table 1 The geographic information of the six automatic weather stations over the TP during GAME-Tibet, numbers in brackets denote the NCEP/NCAR reanalysis values at the nearest grid points

Station	Lhasa	Rikeze	Nagqu	Lingzi	Gaize	Shiquanhe
Longitude (E)	91°08′ (91°53′)	88°53′ (88°08′)	92°04′ (91°53′)	94°28′ (93°45′)	84°25′ (84°45′)	80°05′ (80°57′)
Latitude (N)	29°40′ (29°31′)	29°15′ (29°31′)	31°29′ (31°26′)	29°34′ (29°31′)	32°09′ (31°26′)	32°30′ (33°20′)
Altitude (m)	3649 (3903)	3836 (4056)	4507 (4717)	2991 (3745)	4415 (4754)	4278 (4469)
Topography	Valley	Basin	Plateau	Valley	Plateau	Valley
Environment	City	Suburb	Countryside	Countryside	Countryside	Town

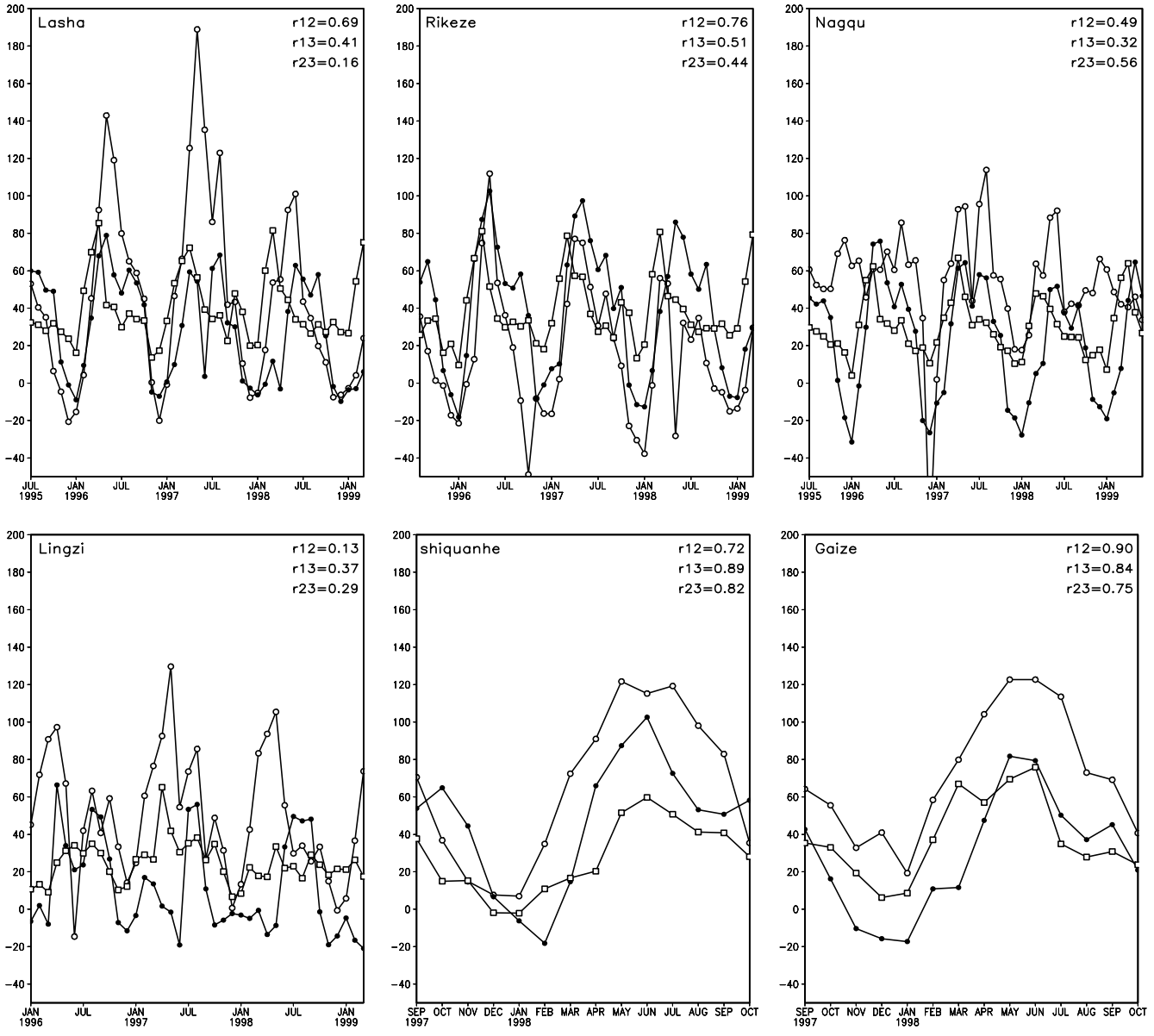

Fig. 1 Series of sensible heat (SH) flux obtained from AMS observation (*open circles*), and NCEP/NCAR (*closed circles*) and ECMWF (*open squares*) reanalysis at the six stations over the TP in units of W m^{-2}, r_{12}, r_{13}, and r_{23} at the top-right corner of each panel represent the correlation coefficients between the time series of AMS and NCEP/NCAR, AMS and ECMWF, as well as NCEP/NCAR and ECMWF, respectively

winter to summer and reaches a maximum (roughly 120 W m^{-2}) in July, then decreases gradually to a minimum (around −80 W m^{-2}) in December, with an annual range of about 200 W m^{-2}. From April to September, the air column over the TP is a heat source but turns into a heat sink during the rests of the year; yet for the annual mean, the atmosphere over the TP is still a heat source. The uppermost contribution to the summer (JJA) total diabatic heating comes from LH, which is nearly triple to that of SH. On the other hand, radiation cooling (RC) always tends to make the air column a heat sink and keeps its intensity around −90 W m^{-2}. These results are basically consistent with the earlier results given by Yeh and Gao (1979), Yanai et al. (1992), and Zhao and Chen (2001). The main difference is that the July mean total diabatic heating of NCEP/NCAR is roughly one third larger than Q_1 given by Yeh and Gao (1979) and Zhao and Chen (2001), but accords with the situation in 1979 shown in Fig. 12 of Yanai et al. (1992). Since the strongest diabatic heating over the TP appears in July, we choose it as a representative of the whole summer in the following parts of this paper.

The horizontal distribution of the July mean column-integrated total diabatic heating and its components over Asia are given in Fig. 4a–d. The boxes ***A***, ***B***, and ***C*** denote TP areas, central Asia (55°–70°E, 30°–42.5°N), and East China (110°–120°E, 27.5°–37.5°N). One can see LH is dominant over the central, southern, and

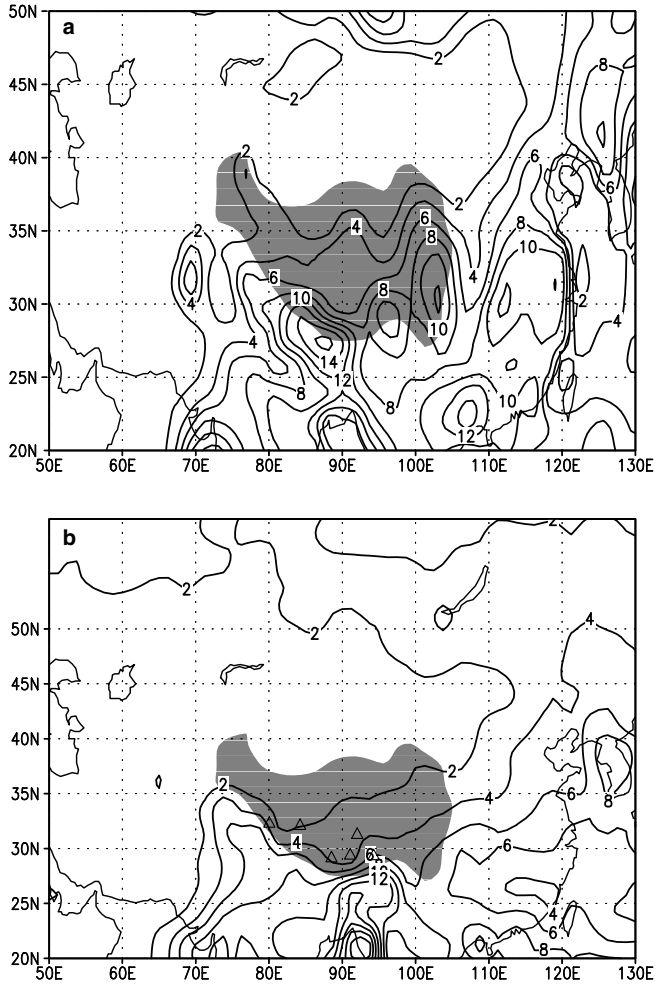

Fig. 2 July mean precipitation over East Asia during 1978–1998. **a** NCEP/NCAR **b** Xie-Arkin. The contour interval is 2 mm day^{-1}. The *shaded area* indicates where the elevation of Tibetan Plateau is higher than 3000 m and the *triangle* in b denotes the location of six AMS

eastern TP and East China, while SH is comparable to or only slightly weaker than LH over the western TP but stronger over its northern flank and over region ***B***. On the other hand, RC with the intensity of -100 W m^{-2} appears over central Asia and exceeds SH over the main body of the plateau. However, owing to the stronger SH, the air column over central Asia is still a weak heat source. In addition, unlike over East China, the atmospheric heating source over the TP should not simply be attributed to monsoon precipitation, because SH is also important in affecting its amplitude and distribution. Particularly as discussed in Sec. 2, SH is likely underestimated but precipitation is overestimated in the NCEP/NCAR data. Comparing Fig. 4d with Q_1 presented in some earlier results (e.g., Fig. 10 in Yanai et al. 1992; Figs. 1–4 in Yanai and Tomita 1998; Fig. 4 in Ueda et al. 2003), there is considerable similarity of the summertime heat source over the TP both in intensity and distribution.

To understand the vertical distribution of summer diabatic heating over the TP and its vicinity, Fig. 5a–c shows the area-averaged total diabatic heating and its individual components (SH, LH, and RC) over the same regions as marked in Fig. 4. In the lower layers over the TP (Fig. 5a), vertical diffusion, with the maximum of more than 10 K per day near the surface, is the primary component of the total diabatic heating and decreases sharply to zero at $\sigma = 0.8$. LH is only half of SH in the surface layers, but exists even in the upper troposphere. Since the intensity of RC is not enough to balance either the low-level SH or mid- and high-level LH, this leads to a huge elevated strong atmospheric heat source with the strongest heating in the surface layers. To the west side of the TP (Fig. 5b), however, LH is almost negligible in the whole troposphere, in accordance with the sparse rainfall there as shown in Fig. 2. The combination of SH and RC, therefore, makes a heat source in the lower troposphere but a weak heat sink above it. In the East Asian region ***C*** (Fig. 5c), deep condensation heating becomes dominant with the upper-layers LH over 3 K per day, whereas the SH and RC are much weaker. Therefore, the diabatic heating profile is characterized by intense SH and LH over the TP, deep LH over East China, and strong surface SH and upper-level RC over central Asia.

4 Corresponding summertime circulation pattern

4.1 Thermodynamic balance

Following the discussions of He et al. (1987), Yanai et al. (1992), and Rodwell and Hoskins (1996, 2001), the

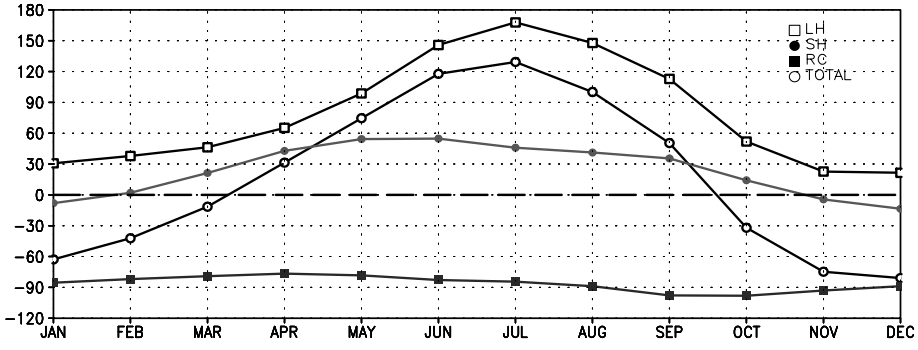

Fig. 3 Climate mean (1980–1999) annual cycle of the area-averaged individual and total diabatic heating over the TP (75°–105°E, 27.5°–37.5°N). Unit is W m^{-2}

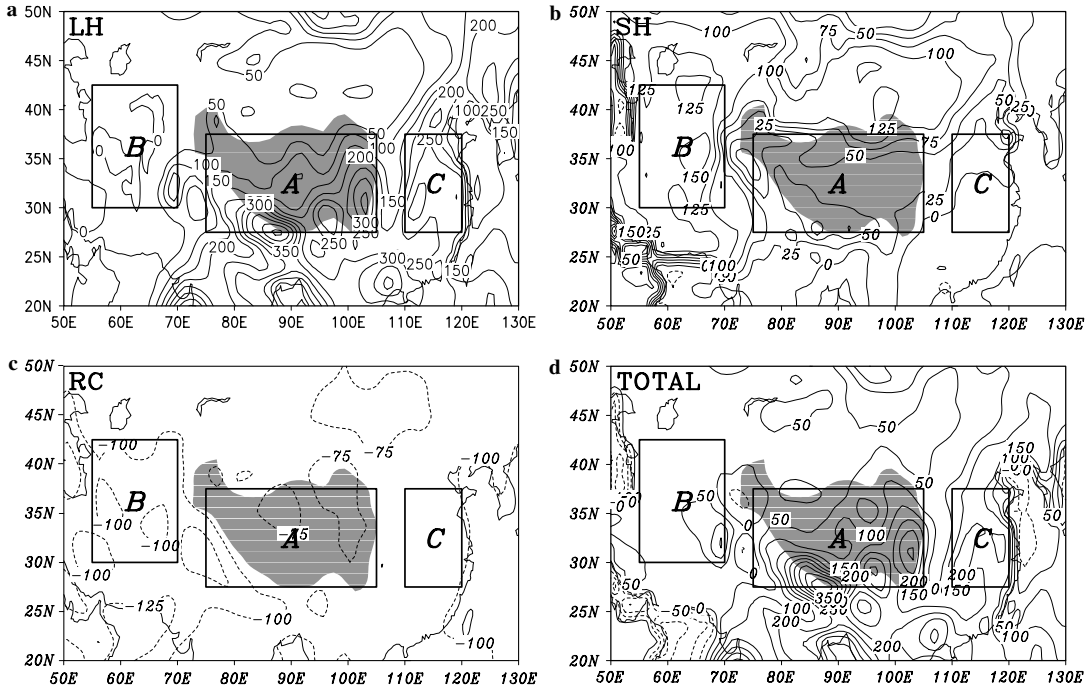

Fig. 4 July mean column-integrated condensation heating LH (**a**), diffusive sensible heating SH (**b**), longwave radiative cooling RC (**c**), and total diabatic heating (**d**) over East Asia. The contour intervals are 50 W m^{-2} in (a) and (d), and 25 W m^{-2} in (b) and (c). The shaded is the same as that in Fig. 2. The boxes **A**, **B**, and **C** denote the areas of Tibetan Plateau, middle Asia, and East Asia, respectively

time-averaged thermodynamic energy equation in pressure coordinates can be written as

$$\underset{\mathrm{A}}{\frac{\partial \overline{T}}{\partial t}} = \underset{\mathrm{B}}{\frac{\bar{Q}}{C_p}} - \underset{\mathrm{C}}{\left(\frac{p}{p_0}\right)^{\kappa} \bar{\omega} \frac{\partial \overline{\vartheta}}{\partial p}} - \underset{\mathrm{D}}{\bar{V} \cdot \nabla_p \bar{T}} - \underset{\mathrm{E}}{\left(\frac{p}{p_0}\right) \frac{\partial}{\partial p} \left(\overline{\omega' \vartheta'}\right)} - \underset{\mathrm{F}}{\nabla_p \cdot \left(\overline{V' T'}\right)} \tag{1}$$

where T is temperature, t is time, C_p is the specific heat of dry air at constant pressure, p is pressure, $\kappa = R/C_p$, R is the gas constant for dry air, ω is vertical velocity and equals to Dp/Dt, $\vartheta = (p/p_0)^{-\kappa} T$ is potential temperature, and V is horizontal wind velocity. An overbar implies a time mean, and a prime signifies deviation from the time

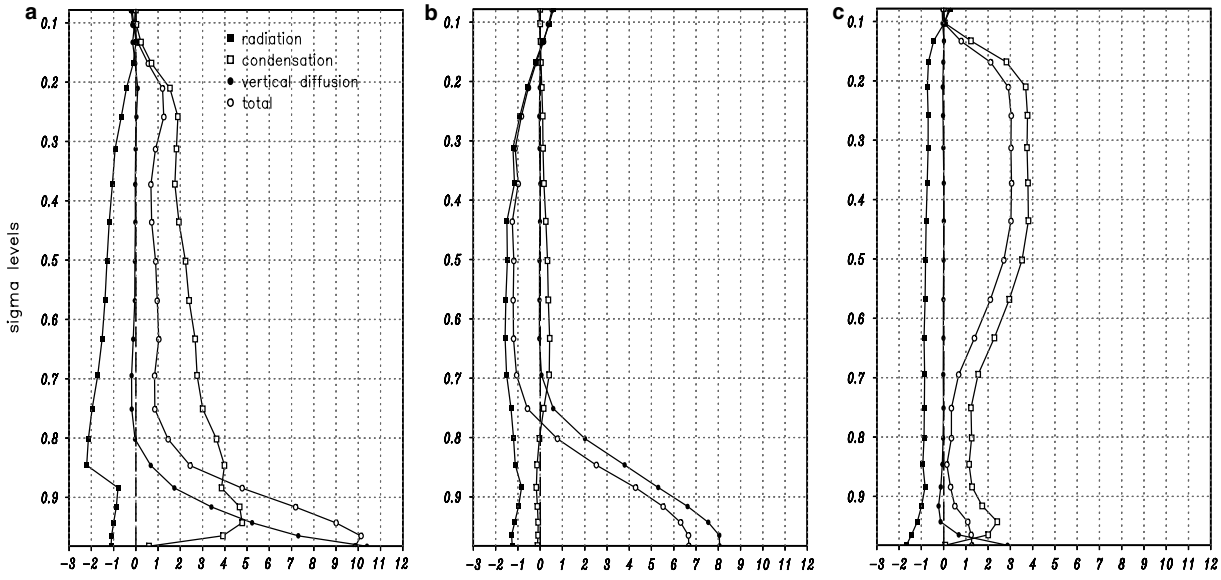

Fig. 5 July mean area-averaged profiles of the total diabatic heating rate and its components over **a** the TP region ***A***,**b** Middle Asia region ***B***,**c** East China region ***C*** as marked in Fig. 4. Unit is K day^{-1}

mean. On the monthly or seasonal time scale, the time tendency term, A, is negligible. For the present study, the July mean NCEP/NCAR climatology from 1980 to 1999 is used to calculate terms C–F, and term B is derived as a residual. At the horizontal grid resolution of 2.5°×2.5°, and particularly away from the midlatitude storm tracks, the transient terms, E and F, do not play a significant role in the balance. Hence the dominant balance is between the diabatic forcing, B, the mean "vertical advection of ϑ", C, and the mean horizontal advection, D.

Figure 6a shows the July mean vertical velocity ω at 400 hPa. Figure 6b–d shows the three terms B, C, and D, respectively, for this period and for the same level. In subtropical Asia, vertical advection C (Fig. 6c) is most important in the thermodynamic balance, while horizontal advection D (Fig. 6d) is only significant over and to the west side of the TP. Exact cancellation between the vertical advection term and the horizontal advection term would imply vertical motions as air moves along sloping isentropic surfaces. Since, in the subtropical descent regions, the diabatic forcing term B (Fig. 6b) and horizontal advection terms are of the same sign rather than tending to cancel, the fraction of the total time-mean descent, which can be directly related to adiabatic motions, could be argued to be approximately D/C, as defined in Eq. 1. Using this argument, it can be seen from diagnosing results shown in Fig. 6 that about 75% of the total descent in region ***B*** to the west of the TP could be expected to result directly from external forcings such as the TP and Asian monsoon, and the remainder to result from the local RC. As a matter of fact, we repeated this analysis at every level and find that the "adiabatic" subsidence in the mid- and upper-layers between 700 and 300 hPa accounts for more than half of the total amount. At 300 hPa, all of the subsidence is "adiabatic" (figures omitted). For the averaged status of the whole air column, therefore, "adiabatic" descent is dominant, in agreement with the results of He et al. (1987) and Yanai et al. (1992), in which they attributed this descent to the vertical circulation induced by the TP. In contrast, the predominant balance over region ***C*** to the east of the TP is between the diabatic term and the mean vertical advection term, just like in the tropics. The strong ascent and condensation heating in region ***C*** are due to the development of monsoonal southwesterlies in East Asia, which are closely related with the TP forcing as will be discussed in the following section. Results from the above diagnosis therefore imply that the thermodynamic balances in region ***B*** to the west of the TP and in region ***C*** to its east are closely related with the TP forcing.

In lower layers of the summer subtropics, since the horizontal advection is not so important, the diabatic warming or cooling $\bar{Q}/c_p$ is always balanced by adiabatic upward or downward motion $(p/p_0)^{\kappa}\,\omega\,\partial\vartheta/\partial p$. As seen in Fig. 5a, b, strong SH with the intensity of more than 8 K per day exists in the surface layers of the TP and to its west side, which must be compensated byadiabatic upward air motion, as will be seen from Fig. 8a. Over the

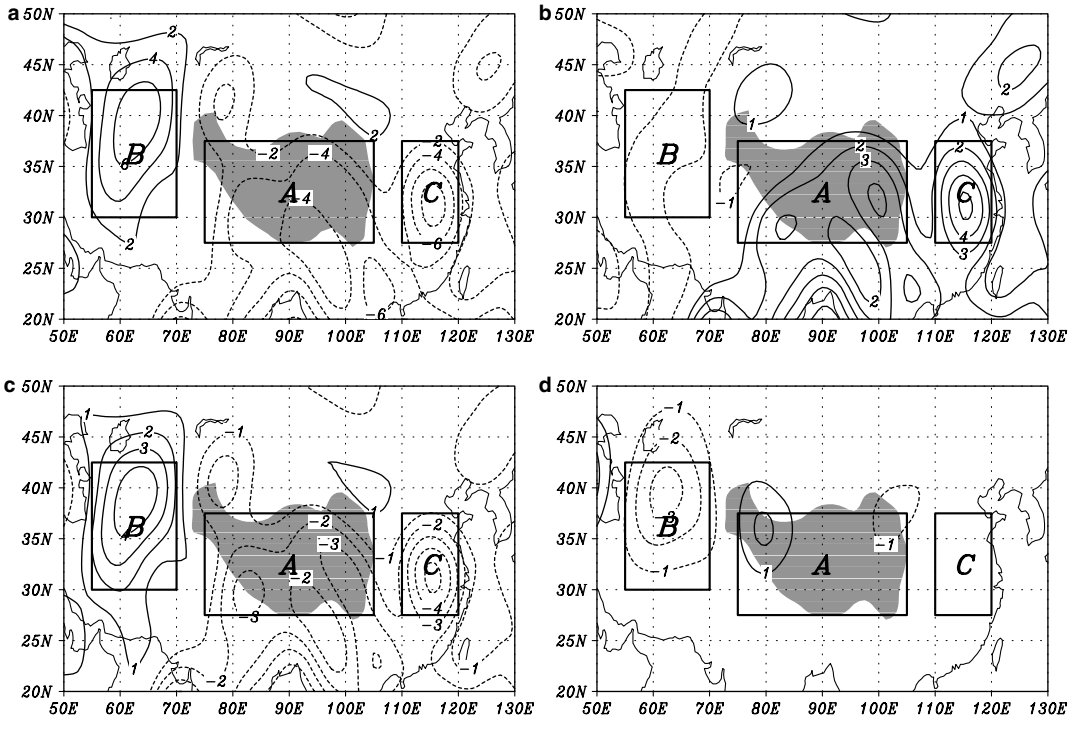

Fig. 6 July means at 400 hPa of **a** Vertical velocity ω (interval is 2×10^{-2} Pa s^{-1}) and the terms in the thermodynamic Eq. 1 (interval is 1 K day^{-1}), **b** Diabatic heating $\bar{Q}/c_p$, **c** Vertical advection $-(p/p_0)^{\kappa}\bar{\omega}\partial\bar{\vartheta}/\partial p$. **d** Horizontal advection $-\bar{V}\cdot\nabla_p\bar{T}$. The *shaded area* indicates where the elevation is higher than 3 Km

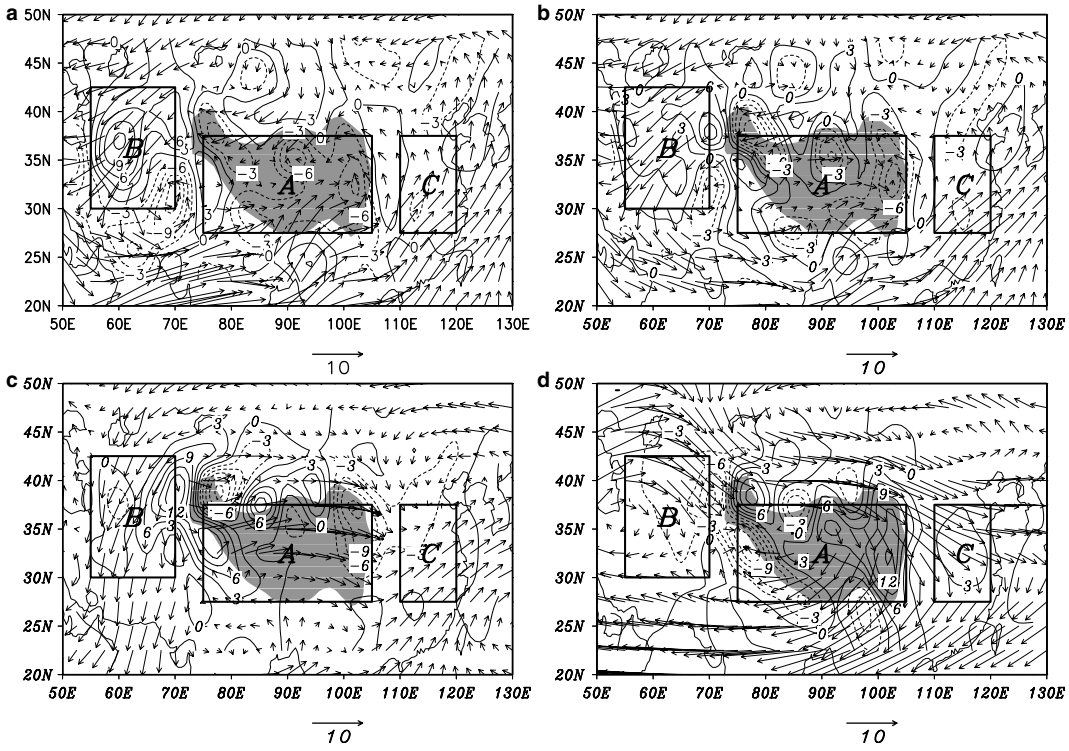

Fig. 7 July mean divergence (contour interval is 3×10^{-7} s^{-1}) and the horizontal wind (unit is m s^{-1}) deviated from zonal mean at **a** Surface-level ($\sigma=0.93$), **b** Low-level ($\sigma=0.81$), **c** Mid-level ($\sigma=0.5$) and **d** Upper-level ($\sigma=0.19$). The *shaded area* is the same as that in Fig. 2

east side, however, owing to insignificant low-level diabatic heating (Fig. 5c), the ascending motion in the lower layers is very weak. Furthermore, the adiabatic descent over central Asia will inhibit local convective heating and increase long-wave cooling thus leading to a local "diabatic enhancement" (Rodwell and Hoskins 2001). Similarly, deep convective heating over East China is in favor of the in situ ascending motion. Thus, there could be positive feedbacks between the vertical motion and local diabatic heating.

4.2 Circulation and vertical motion

In work investigating the features of atmospheric motion as a result of diabatic heating, Hoskins (1991) and Wu and Liu (2000) have brought forward the thermal adaptation theory based on a PV-ϑ view. The main idea is that the thermal forcing of diabatic heating increases the potential temperature of the air column, and the induced mechanical forcing results in convergence in lower layers but divergence in upper layers. Lower layer cyclonic circulation and upper layer anticyclonic circulation are formed. For a strong near surface heating, the low-layer isentropic surfaces descend sharply and intersect the ground surface along the boundary of heating. Huge negative vorticity is then created due to surface friction and pumped into the air column, forcing deep-layer anticyclonic circulation above the lower-layer cyclonic circulation. As revealed earlier, in summertime SH is primary in lower layers over the TP but LH is overwhelming in the higher layers. This type of vertical nonuniform heating therefore generates a shallow and weak low in the surface layers but a deep and strong high above it (Li WP et al. 2001; Liu X et al. 2001; Liu YM et al. 2001). Such an out-of-phase feature in circulation will result in different vertical velocity between the west and east sides of the TP.

The July mean horizontal wind vector as well as divergence fields at various levels in a σ-coordinate is shown in Fig. 7a–d, noting that $\sigma=0.9$ and $\sigma=0.1$ roughly represent the levels of 540 and 60 hPa over the TP. Near the surface (Fig. 7a), surrounding cyclonic airflows move towards the midst of the TP and converge there (denoted by a negative contour value), and region ***B*** to the west of the TP is characterized by equatorward prevailing wind and divergent airflow (denoted by a positive value). However, the situation is completely reversed over region ***C*** to the east of the TP with convergent airflows and the low-level southwesterly jet, which is a member of the summer monsoon system over East Asia. Such a pattern remains in the lower layer $\sigma=0.81$ (Fig. 7b), with the divergence center over central Asia becoming weaker. At the mid troposphere (Fig. 7c), however, air flows out and becomes divergent over the western TP, whereas there is no obvious change in regions ***B*** and ***C*** to both its west and east sides. In reaching the upper troposphere (Fig. 7d), the circulation pattern over subtropical and tropical Asia is totally different than its counterpart in lower layers. Over the

TP region is an anticyclonic circulation system with strong divergence, over region ***B*** is another anticyclone but with convergence. These two anticyclones correspond to the bimodality of the summertime South Asian High as reported by Zhang et al. (2002). Over region ***C*** are equatorward meridional wind and air divergence.

The corresponding vertical velocity fields are shown in Fig. 8a–d, in which positive and negative values denote descending and ascending motions, respectively. In the surface layers of subtropical and tropical Asia (Fig. 8a), besides the ascending motion over the plateau, there are three localized summertime ascending centers in the vicinity of the TP. The strongest one is centered over the south fringe of the TP, in accordance with the in situ rainfall center shown in Fig. 2. The west-side center at about (65°E, 37°N) is located over the Kyzylkum desert region in central Asia. A third center occurs over the north side of the plateau. These two surface-rising centers are associated with the low-level SH. With the increasing height, all of these ascending centers decrease gradually. At the level of $\sigma = 0.81$ (Fig. 8b), most areas in region ***B*** is replaced by downward motion with the center moving westward somewhat, in accord with the in situ RC; whereas, the ascending centers over both the north and south sides of the TP remain stable. In the mid layers (Fig. 8c), upward motion over the north side disappears and the south side ascending center no longer exists. Meanwhile, a new ascending region, centered at the position of (117°E, 32°N), appears over region ***C*** and remains until reaching the tropopause (Fig. 8d). It is notable that upward motion in the surface layers is generated by different external forcings over the south and west sides of the TP. To the south fringe of the TP, due to the steep orography, moist airflows arising from tropical oceans are uplifted along the slopes and result in vigorous ascending motion and corresponding abundant rainfall. However, due to milder orography in the west flank of the TP, the uplifting effect is much weaker, and the SH is responsible for the surface ascending motion but RC above it prohibits the vertical development of the ascending motion in the upper layers.

5 Impacts of the TP thermal forcing on the Asian climate

The atmospheric response to a thermal forcing can be well explained by the following Ertel potential vorticity (PV) equation (Ertel 1942):

$$\frac{\mathrm{d}P}{\mathrm{d}t} = \alpha\vec{F}\cdot\nabla\vartheta + \alpha\vec{\zeta}_a\cdot\nabla Q, \tag{2}$$

where $\vec{\zeta}_a$ is absolute vorticity; Q, diabatic heating; $\vec{F}$, frictional dissipation of $\vec{\zeta}_a$; and P, the Ertel vorticity.

$$P = \alpha\vec{\zeta}_a\cdot\nabla\vartheta. \tag{3}$$

By using the related PV-ϑ view, Hoskins (1991) interprets the atmospheric response to a given thermal forcing as the formation of lower layer cyclonic circulation and upper layer anticyclonic circulation. From the last term on the right hand side of (2), it can be referred that the vertical scale of such a solely thermal response depends greatly on the vertical scale of diabatic heating. This becomes evident in the analytical as well as

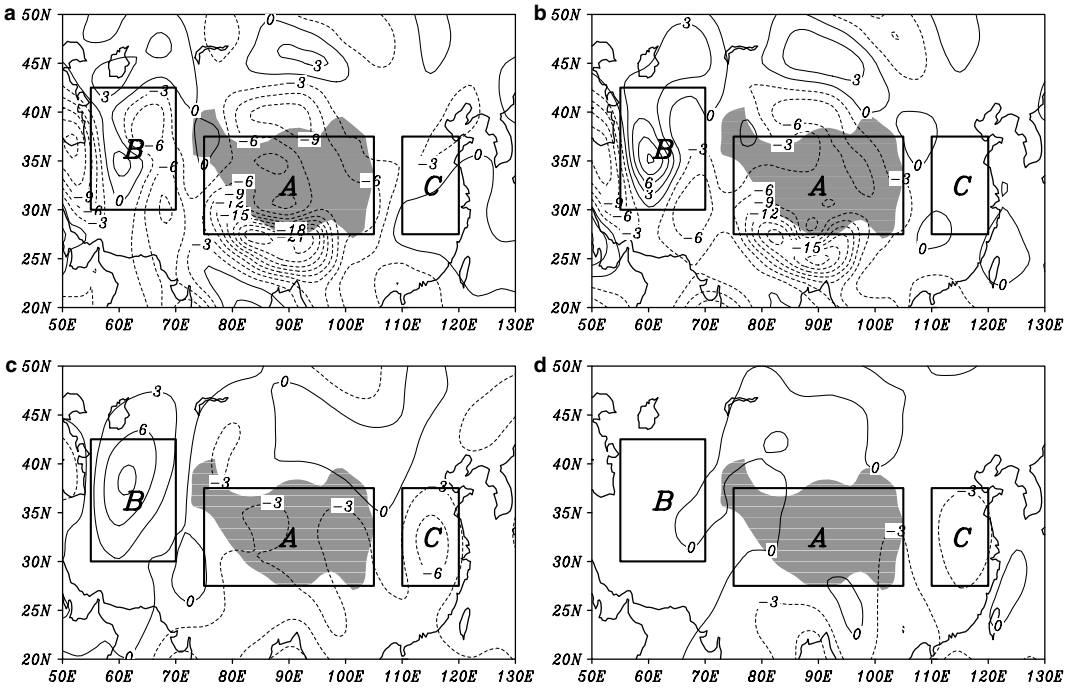

Fig. 8 The same as in Fig. 7 except for July mean vertical velocity. The contour interval is 3×10^{-2} Pa s^{-1}

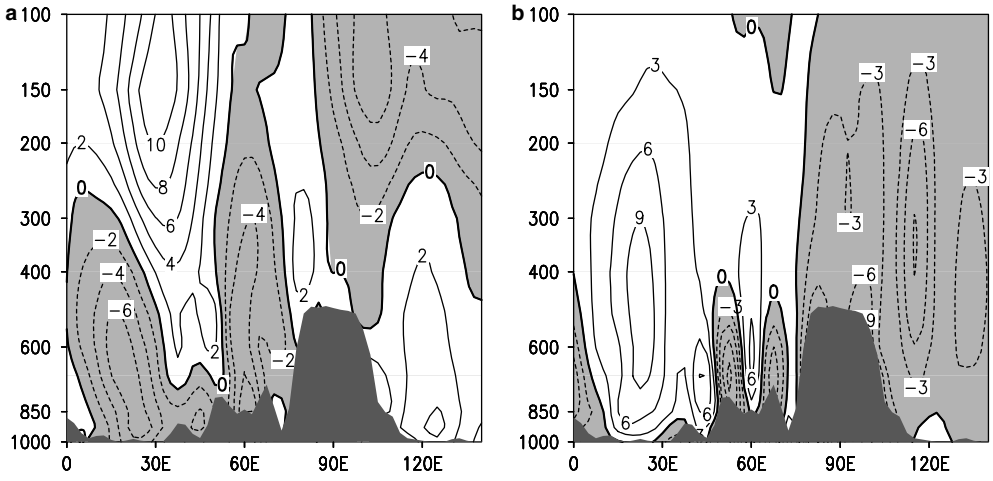

Fig. 9 Longitude–pressure sections of July mean **a** Meridional wind **b** Vertical velocity along 32.5°N in *p*-coordinates. The contour intervals are 1 m s^{-1} in (a) and 2×10^{-2} Pa s^{-1} in (b)

numerical studies of Wu (2003) on the circulation response to a prescribed deep/shallow convective-type heating. The height of forced vertical velocity (his Fig. 4) and perturbation temperature (his Fig. 5) closely follows the height of the given heating in either the deep or the shallow convective heating cases.

The thermal adaptation theory developed by Wu and Liu (2000, also Wu et al., personal communication) extends the PV-ϑ view of Hoskins by taking into account the impacts of surface friction (Fig. 3 of Wu et al. 2004). For a near surface heating source, its warming to the atmosphere causes the intersection with the earth's surface of the lower-layer isentropic surfaces. Negative vorticity induced by surface friction ($\alpha\vec{F}\cdot\nabla\vartheta<0$ in Eq. 2) is pumped into the air column, diluting the lower layer positive vorticity, due to heating, and extending the anticyclonic circulation aloft to the upper troposphere. Using a simple β-plane nonlinear model with Rayleigh friction and assuming a vertically exponential-decreasing heating with a maximum heating of 1.4 K d^{-1} at the surface, Wang et al. (1996) obtained a strong and shallow cyclone in the lower layers and weak and deep anticyclone in the upper layers up to 10 Km in the subtropics (their Fig. 11g, h and Fig. 12 g, h). In summer along subtropical continent or over the TP, surface heating rate of about 10 K d^{-1} (or 100 W m^{-2}) is common. By placing two continental-scale subtropical surface SH flux of 100 W m^{-2} onto the surface of an aqua-planet in mimicking the Eurasian and North American Subtropical continental SH demonstrated that such a simple heating model captures the main features of the summertime subtropical circulations; two shallow anticyclones with reasonable amplitude are over the two "ocean " surface. Two shallow cyclones and two deep anticyclones are over the heating areas. All these experimental results support the theory that due to surface friction, the atmospheric thermal adaptation to a surface heating is producing shallow cyclone in the lower layers and deep anticyclone in aloft.

To reveal the vertical structure of the circulation demonstrated in Fig. 7 and the vertical motion demonstrated in Fig. 8. Figures 9a, b are presented the July mean pressure–longitude cross sections of the meridional wind component and vertical velocity along 32.5°N. Over the Tibetan Plateau sector between 75° and 105°E and the Iran Plateau sector between 40° and 75°E, the meridional wind fields (Fig. 9a) are characterized with anticyclonic circulations in the deep upper troposphere but cyclonic circulation near the surface. This circulation pattern is nested in the continental scale circulation pattern with southerlies on its east and northerlies on its west in the lower troposphere and a corresponding out-of-phase structure in the upper troposphere. The two zero isolines near 60° and 90°E represent the bimodality of the South Asian High as shown in Fig. 7d. As discussed earlier, the atmospheric adaptation to a thermal forcing is to generate cyclonic circulation in lower layers and anticyclonic circulation in the upper layers. The vertical structure of the circulations between 40° and 75°E and between 75° and 105°E is associated with the thermal forcing over Iran Plateau (Zhang et al. 2002) and the TP (Wu 2004; Wu et al. 2004), respectively; whereas the lower tropospheric continental cyclonic circulation with northerlies to the west of 40°E and southerlies to the east of 105°E and the continental scale anticyclonic circulation aloft are forced by the LO-SE-CO-D quadruplet heating (Wu and Liu 2003) as mentioned in Sec. 1. Following a simple vorticity balance argument, since the advection of relative vorticity in the summer subtropics is weak, the time-mean quasi-geostrophic vorticity equation for large-scale air motion in the subtropics can be written as

$$\beta v + (f+\zeta)\nabla\cdot\vec{V} = 0 \qquad (4)$$

in which β and f are Rossby and Coriolis parameter, v is meridional wind speed, ζ relative vorticity, and $\nabla\cdot\vec{V}$ air divergence. The vertical structure of the circulation produced by a heating should have lower-layer convergence and upper-layer divergence on its eastern side, and lower-layer divergence and upper-layer divergence on its western side. Following a continuity requirement argument, therefore, the vertical shear of meridional wind over a heating source along subtropics should corre-

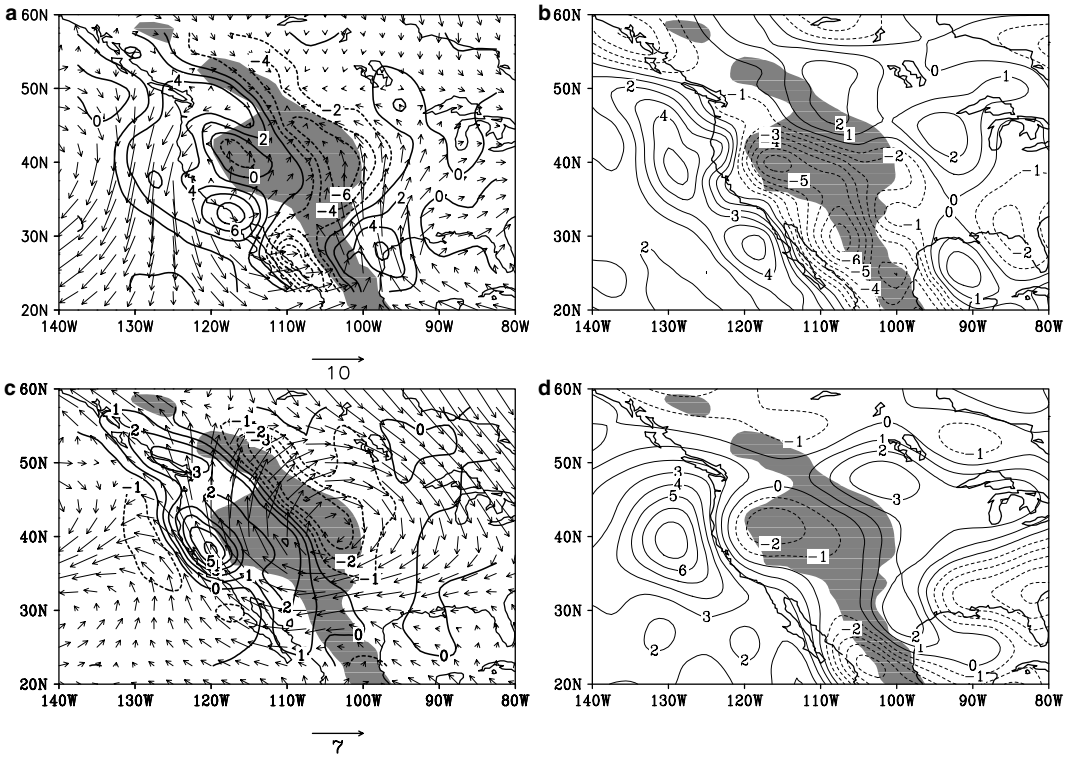

Fig. 10 July mean divergence and horizontal wind deviated from zonal mean (**a, c**), and vertical velocity (**b, d**) at the surface-level $\sigma = 0.93$ (**a, b**) and the mid-level $\sigma = 0.5$ (**c, d**). Units are m s^{-1} for wind speed and 1×10^{2} Pa s^{-1} for vertical velocity; the divergence contour intervals are 2×10^{-7} s^{-1} in (a) and 1×10^{-7} s^{-1} in (c). The shaded area denotes the regions where the altitude is greater than 1000 m

spond to ascending motion on its east but descending motion on its west. This is the case as presented in Fig. 9b. Corresponding to the mountain crests at 50°, 70°, and 90°E, there exist three pairs of descent/ascent in the lower troposphere with ascent over the crests and their eastern sides. The continental scale vertical motion also corresponds to ascent on the east and descent on the west. The ascending motion over the eastern continent and the descending over its west induced by continental heating are at least partly overlapped with those induced by large-scale orographic thermal forcing. Therefore, the existence of the TP and Iran Plateau reinforces the East Asian monsoon rainfall to their east and enhances the dry and hot climate in central and western Asia to their west. These results are in agreement with those based on the sensitivity numerical experiments with and without the TP (e.g., Hahn and Manabe 1975; Liu and Yin 2002),.

6 Comparison of summertime circulation patterns over the global subtropical large-scale mountains

A fluid dynamical difference between the effects of the TP and those of the Rocky and Andes Mountains should be pointed out here immediately. For the north–south oriented Rockies and Andes, the basic westerly flow goes over the mountain, but for the west–east oriented the TP, the basic westerly flow goes around the TP. The classical linear formulation of the lower boundary condition is suitable only for the former, Chen and Trenberth (1988a, 1988b) and Trenberth and Chen (1988) improved the lower boundary condition to allow the flow to "circumvent" the TP. Some other differences such as height, width, outline, slope, and geographical location have been documented in Tang and Reiter (1984). Despite all these differences, the Rocky and Andes Mountains also act as large-scale heating sources in summer; hence the explanation for the summer climate patterns over both the west and east sides of the TP should be applicable to the Rocky and Andes Mountains.

Following the same analysis routine as in Sect. 4, Fig. 10 shows the July mean wind vectors and divergence, as well as the vertical velocity in the lower layer ($\sigma = 0.93$) and mid layer ($\sigma = 0.5$) over the Rocky Mountains. There is strong air convergence over the mountain ranges in the lower layer, and a cyclonic circulation exists in the wind deviation from the zonal mean (Fig. 10a), accompanied by equatorward and poleward flows prevailing on its west and east sides. In the corresponding vertical velocity field (Fig. 10b), the summer descent regions to the west of the Rockies are located off the coastal regions of California, with two centers located at (128°W, 40°N) and (119°W, 28°N), respectively. To the east of the Rockies, two other

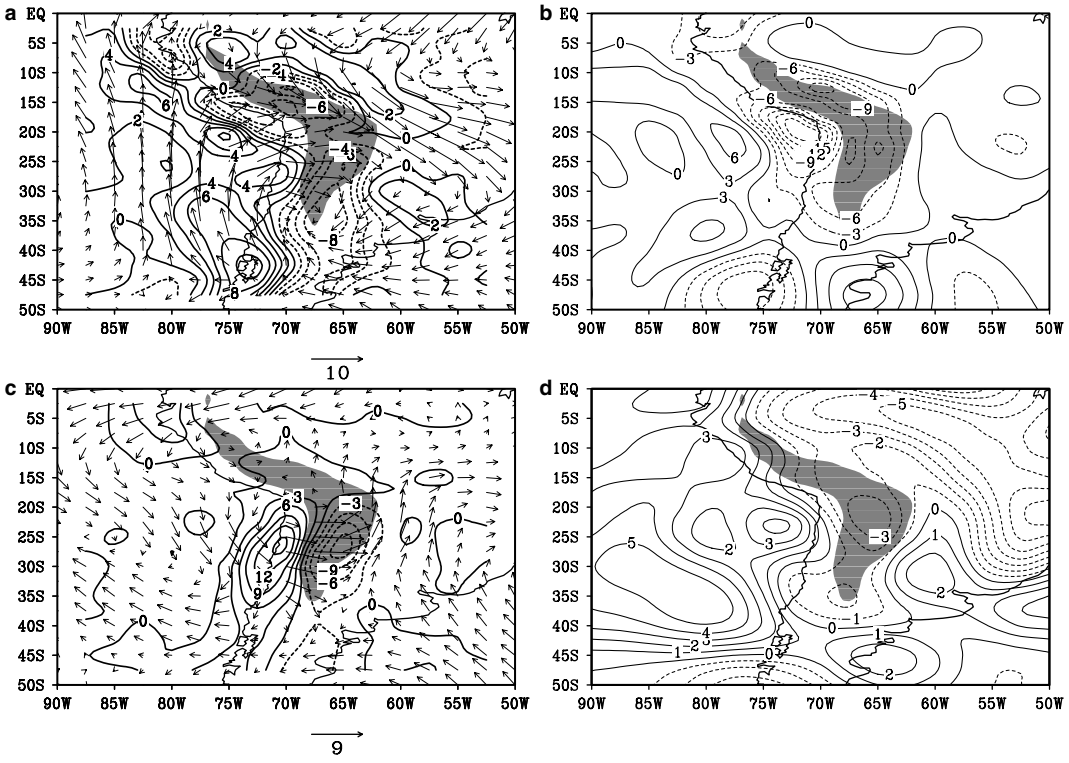

Fig. 11 The same as in Fig. 10 except for January means. Unit of wind speed is in m s^{-1}. The contour intervals are 2×10^{-7} s^{-1} and 3×10^{-7} s^{-1} for divergence in (a) and (c), and 3×10^{2} Pa s^{-1} and 1×10^{2} Pa s^{-1} for vertical velocity in (b) and (d), respectively. The shaded area denotes the regions where the altitude is greater than 1500 m

descending centers lie in 25° and 45°N at the longitude of about 90°W. However, uniform ascending motion can be observed over the mountains. It is somewhat different than the TP situation in that a reversed anticyclonic circulation appears in mid layers (Fig. 10c) rather than in upper layers, and this may be interpreted by the lower elevation and the weaker heat source in the lower layers. In the corresponding divergence field, parts of the low-level air divergence over the East Pacific have been replaced by convergence, but the diverging center over the western flank of the mountains and the converging center to its east still remain there. Since $\sigma = 0.5$ near the level of non-divergence over the plain areas, the zero contour of $\nabla \cdot \vec{V}$ covers most parts of eastern North America. On the other hand, a typical Rossby wave train propagating eastward and poleward can be found in the corresponding ω field (Fig. 10d), denoting that the circulation in mid-latitudes is also affected by the large-scale orography-related thermal forcing through the propagation of Rossby waves. Since the diabatic heating is mainly dependent on SH over the subtropical and mid latitude parts of the Rockies (figures not shown), and since the mountain range has a lower altitude of orography than the TP, the heating center is always located at the central part of the terrain in higher latitudes within westerlies. This is at least a partial reason why the corresponding circulation center over the Rocky Mountains appears in the mid latitudes rather than the subtropics.

The situation over the summertime Andes Mountains is similar, only with the circulation center slightly displaced equatorward (Fig. 11a–d). The low-level ($\sigma = 0.93$) cyclone, accompanied with air convergence, controls most parts of the South America continent as well as the adjacent oceans. The mid-level ($\sigma = 0.5$) anticyclone above it has a smaller domain, accompanied with an air convergence center over the subtropical mountains and a divergent center to its west. In the corresponding vertical motion field, there is uniform ascending in low-level, with two centers located at the tropical Andes and the south Pacific. In mid-level, the ascending center changes to the descending center over the ocean and the continental ascending center moves to the middle of the Andes.

Thus the basic circulation feature over the global subtropical mountains can be generalized as follows: a cyclonic circulation, accompanied by strong air convergence and subsequent upward motion over the terrain, controls the lower troposphere, and an anticyclonic circulation stands in the higher layers. In the corresponding horizontal wind and vertical motion fields, the west side of the mountain is characterized by equatorward airflow in lower layers and a reversed distribution in higher layers with descending motion in the free atmosphere, whereas the east side is characterized by poleward prevailing airflow and ascending motion in lower layers and equatorward airflow in upper layers. Moreover, some significant differences between the TP

on one hand and Rockies and Andes on the other can be observed. Because the TP is located to the east of the Eurasian continent, its thermal impacts are to enhance southwesterlies, atmospheric ascent and East Asian monsoon to its east, as well as northerlies, atmospheric descent and dryness to its west. On the other hand, since the Rocky and Andes are located at the west of North and South America, respectively, the western part of the low-level cyclone and high-level anticyclone induced by continental-scale summer subtropical heating overlaps with its counterpart induced by mountain heating, thus leading to a strong equatorward airflow and the in situ adiabatic descent. Since the descent occurs over the eastern Pacific ocean, it does not correspond with underlying desert as the TP does. Instead, the positive feedback between the intense RC above the anomalously cold SSTs (Klein and Hartmann 1993; Klein et al. 1995; Ma et al. 1996) and the vertical motion further enhances the local diabatic descent, forming stable boundary layers stratus cloud to the western coasts of North and South America and the strong in situ atmospheric cooling (referred to Fig. 2 of Rodwell and Hoskins 2001 and Fig. 1 of Wu and Liu 2003). Furthermore, the mountain induced ascending motion does not connect with the ascending motion induced by continental heating in the subtropics of both North and South America partly due to lee-side descending motion. As a result, the summer monsoon in either North America or South America is not as intense as in Asia.

7 Concluding remarks

The thermal effect of the TP plays an important role in the subtropical climate patterns over summertime subtropical Asia, and this investigation, based on data diagnosis, focuses on the mechanism of how the TP affects the summertime subtropical circulation by its thermal forcing. Since the TP acts as a strong heat source in summer with the strongest heating layer lying in the lower layers, the thermal adaptation results in a shallow and weak cyclonic circulation near the surface and a deep and strong anticyclonic circulation above it. According to the large-scale quasi-steady vorticity equation for the subtropics, airflows along the east flank of the TP therefore must be convergent in lower layers and divergent in upper layers, and the sucking and pumping effects lead to vigorous ascent in situ. As a consequence, the combined effects of large amounts of moisture flux arising from the Tropics and convective motion result in plentiful rainfall over the east flank of the TP. In contrast, along the west of the TP, airflows diverge in lower layers but converge above it, leading to subsidence and the associated northerly flow in lower layers. Hence the effect of the TP thermal forcing is to generate and maintain a Gill type circulation in lower layers and an opposite circulation in upper layers. Similar configuration in meridional wind and vertical motion exist over Iran Plateau except that the vertical ascent only reaches the mid-troposphere, and the upper troposphere is dominated by subsidence. The results of the thermodynamic balance diagnosis indicate that the main part of the subsidence in the free atmosphere to the west of the TP is "adiabatic". This provides further evidence for the role of the TP's thermal and mechanical forcing.

The continental-scale diabatic heating along the summer subtropics generates lower layer cyclonic circulation and upper layer anticyclone circulation over land areas (Wu and Liu 2003; Liu et al. 2004). Therefore the circulation pattern forced by the continental-scale heating over Eurasian is in phase with the circulation patterns forced by the thermal forcing of the TP and Iran Plateau. Therefore, the subsidence over the western continent and the upward motions over its east are enhanced greatly, resulting dry and hot climate in west and middle Asia but strong monsoon and wet climate in East Asia.

The similar summertime circulation configuration also exists over the other subtropical large-scale terrains, such as the Rockies and Andes Mountains, and this reflects the universality of the thermal adaptation theory. On the other hand, due to the different geographical location, local diabatic heating distributions, and orographies, some differences are remarkable. The TP is located over the eastern part of the Eurasian continent, and its thermal forcing greatly intensifies the lower layer southerlies to its east, forming strong East Asian monsoon and bringing abundant rainfall. To its west, strong subsidence occurs over land surface, forming severe deserts. However, the Rockies and Andes are located near the western coasts of continents. The lower-layer poleward flow on their east does not coincide with the poleward flow along the eastern coasts in subtropics, and monsoon climate is weaker. On the other hand, the orographic forcing greatly intensifies the subsidence and surface northerly over the area along and off the western coasts forced by continental heating. Since the intense subsidence occurs over the cold surface of the eastern oceans, no desert is formed. Instead, the intense subsidence over the cold ocean surface leads to strong atmospheric stability in the boundary layer, contributing to the formation of vast low stratus clouds and strong long-wave radiative cooling over the eastern subtropical North Pacific and South Pacific in summer (Wu and Liu 2003).

As discussed by preceding studies (e.g., Zhu 1957a, 1957b; Hahn and Manabe 1975), thermal effects of large-scale mountains are closely connected with their mechanical counterparts. For example, the elevated land surface of the TP obviously enhances the effect of the atmospheric heating source in summer. This is the oneness of the thermal and mechanical effects of large-scale orography on the atmospheric general circulation, which was first defined by Zhu (1957a, 1957b), and these two aspects are closely connected with each other through dynamical processes.

Most recently, Duan et al. (2003) and Hsu and Liu (2003) have investigated the relation between springtime thermal status over the TP and the circulation as well as the rainfall over China in the subsequent summer season. It turns out that when SH over the TP is abnormally strong during spring season, there will be much more rainfall in July over the Yunnan–Guizhou Plateau and the middle reaches of the Yangtze River and Huaihe River. In contrast, rainfall in North and South China will be less than normal. This can be attributed to the persistence of the SH over the TP and the subsequent abnormally strong Gill type circulation above it. Therefore, understanding the effects of the TP thermal forcing is also instructive for improving the short-range climate prediction in East Asia.

However, a more detailed and higher quality dataset is needed to further understand the effects of the TP on the subtropical climate patterns. This work, some of it in progress, will have to rely on numerical modeling to a considerable degree, which will help to test the sensitivity of atmospheric response to certain interaction mechanisms.

Acknowledgements We would like to thank the anonymous reviewers whose critical reviews and valuable suggestions are important for the improvement of the manuscript. The authors also thank Dr. G.P. Li for providing the AMS heat flux data. This work is jointly supported by the Chinese Academy of Sciences (Grant No. ZKCX2-SW-210), and by the National Natural Science Foundation of China (Grant No. 40405016, 40475027, 40135020, and 40221503).

References

Annamalai H, Slingo JM, Sperber KR, Hodges K (1999) The mean evolution and variability of the Asiuabn summer monoon: comparison of ECMWF and NCEP-NCAR reanalyses. Mon Wea Rev 127:1157–1186

Bolin B (1950) On the influence of the Earth's orography on the general character of the westerlies. Tellus 2(3):184–195

Broccoli AJ, Manabe S (1992) The effects of orography on midlatitude Northern Hemisphere dry climates. J Clim 5:1181–1201

Charney JG, Eliassen A (1949) A numerical method for predicting in the perturbation of the middle latitude westerlies. Tellus 1:38–54

Chen SC, Trenberth KE (1988a) Orographically forced planetary waves in the Northern Hemisphere winter: steady state model with wave-coupled lower boundary formulation. J Atmos Sci 45:657–680

Chen SC, Trenberth KE (1988b) Forced planetary waves in the Northern Hemosphere winter: wave-coupled orographic and thermal forcings. J Atmos Sci 45:682–704

Döös BR (1962) The influence of the exchange of sensible heat with the earth's surface on the planetary flow. Tellus 14:133–147

Duan AM (2003) The Influence of Thermal and Mechanical Forcing of Tibetan Plateau upon the Climate Patterns in East Asia. Ph.D. thesis, Institute of Atmospheric Physics, Chinese Academy of Sciences, 161pp

Duan AM, Liu YM, Wu GX (2003) Heating status of the Tibetan Plateau from April to June and rainfall and atmospheric circulation anomaly over East Asia in midsummer (in Chinese). Sci China Ser D 33(10):997–1004

Ertel H (1942) Ein Neuer hydrodynamischer Wirbelsatz. Met Z 59:271–281

Flohn H (1957) Large-scale aspects of the "summer monsoon" in South and East Asia. J Meteor Soc Japan 75:180–186

Flohn H (1960) Recent investigation on the mechanism of the "summer monsoon" of southern and eastern Asia Proc Symp Monsoon of the World. Hindu Union Press, New Delhi, pp75–88

Gill AE (1980) Some simple solutions for heat-induced tropical circulation. QJR Meteorol Soc 106:447–462

Hahn DG, Manabe S (1975) The role of mountains in the south Asian monsoon circulation. J Atmos Sci 32:1515–1541

He HJ, McGinnis W, Song Z, Yanai M (1987) Onset of the Asian summer monsoon in 1979 and the effect of the Tibetan Plateau. Mon Wea Rev 115:1966–1995

Hoskins B (1991) Towards a PV-ϑ view of the general circulation. Tellus 43AB:27–35

Hoskins B, Karoly D (1981) The steady linear response of a spherical atmosphere to thermal and orographic forcing. J Atmos Sci 38:1179–1196

Hsu HH, Liu X (2003) Relationship between the Tibetan Plateau heating and East Asian summer monsoon rainfall. Geophys Res Lett 30(20):2066

Kalnay E, and Coauthors (1996) The NCEP/NCAR 40-year reanalysis project. Bull Am Meteorol Soc 77(3):433–471

Klein SA, Hartmann DL (1993) The seasonal cycle of low stratiform clouds. J clim 6:1587–1606

Klein SA, Hartmann DL, Norris JR (1995) On the relationships among low cloud structure, sea surface temperature and atmospheric circulation in the summertime northeast Pacific. J Clim 8:1140–1155

Koteswaram P (1958) The easterly jet stream in the tropics. Tellus 10:43–57

Li CF, Yanai M (1996) The onset and interannual variability of the Asian summer monsoon in relation to land-sea thermal contrast. J Clim 9:358–375

Li GP, Duan TY, Gong YF (2000) The bulk transfer coefficients and surface fluxes on the western Tibetan Plateau. Chinese Sci Bull 45(13):1221–1226

Li GP, Duan TY, Haginoya S, Chen LX et al (2001) Estimates of the bulk transfer coefficients and surface fluxes over the Tibetan Plateau using AWS data. J Meteorol Soc Japan 79(2):625–635

Li WP, Wu GX, Liu YM, Liu Y (2001) How the surface processes over the Tibetan Plateau affect the summertime Tibetan Anticyclone: numerical experiments (in Chinese). Chinese J Atmos Sci 25(6):809–816

Liu XD, Yin ZY (2002) Sensitivity of East Asian monsoon climate to the Tibetan Plateau uplift. Palaeogeogr Palaeoclim Palaeoecol 183:223–245

Liu X, Wu GX, Li WP, Liu YM (2001) Thermal adaptation of the large-scale circulation to the summer heating over the Tibetan Plateau (in Chinese). Prog Nat Sci 11(3):207–214

Liu YM, Wu GX, Liu H, Liu P (2001) Condensation heating of the Asian summer monsoon and the subtropical anticyclone in the Eastern Hemisphere. Clim Dyn 17:327–338

Liu YM, Wu GX, Ren RC (2004) Relationship between the subtropical anticyclone and diabatic heting. J Clim 17:682–698

Luo H, M Yanai (1984) The large-scale circulation and heat sources over the Tibetan Plateau and surrounding areas during the early summer of 1979. Part II: heat and moisture budgets. Mon Wea Rev 112:966–989

Ma CC, Mechoso CR, Robertson AW, Arakawa A (1996) Peruvian stratus clouds and the tropical Pacific circulation: a coupled ocean-atmosphere GCM study. J Clim 9:1635–1645

Matsumoto J, Shen X, Numaguti A (1999) GAME Large-scale monitoring for the Intensive Observation Period, April–September 1998. GAME Publ. 12, Center for Climate System Research, University of Tokyo, Japan,540 pp

Murakami T (1958) The sudden change of upper westerlies near the Tibetan Plateau at the beginning of summer season (in Japanese). J Meteor Soc Japan 36:239–247

Rodwell MJ, Hoskins BJ (1996) Monsoon and the dynamics of deserts. QJR Meteorol Soc 122:1385–1404

Rodwell MJ, Hoskins BJ (2001) Subtropical anticyclones and summer monsoons. J Clim 14:3192–3211

Smagorinsky J (1953) The dynamical influence of long-scale heat source and sinks on the quasi-stationary motion of the atmosphere. QJR Meteor Soc 79:342–366

Smith EA, Shi L (1992) Surface forcing of the infrared cooling profile over the Tibetan Plateau. Part I: influence of relative longwave radiative hearing at high altitude. J Atmos Sci 49:805–822

Staff Members of the Section of Synoptic and Dynamic Meteorology, Institute of Geophysics and Meteorology, Academia Sinica, Peking (1957) On the general circulation over eastern Asia (II). Tellus 10:58–75

Tang M, Reiter ER (1984) Plateau monsoons of the Northern Hemisphere: a comparison between North America and Tibet. Mon Wea Rev 112:617–637

Tao SY, Ding YH (1981) Observational evidence of the influence of the Qinghai-Xizang (Tibet) Plateau on the occurrence of heavy rain and severe convective storms in China. Wea Forecasting 2:89–112

Trenberth KE, Chen SC (1988) Planetary waves kinematically forced by Himalayan orography. J Atmos Sci 43:2934–2948

Trenberth KE, Guillemot CJ (1998) Evaluation of the atmospheric moisture and hydrological cycle in the NCEP/NCAR Reanalysis. Clim Dyn 14:213–231

Ueda H, Kamahori H, Yamasaki N (2003) Seasonal contrasting features of heat and moisture budgets between the eastern and western Tibetan Plateau during the GAME IOP. J Clim 16:2309–2324

Wang TA, Lin YL, Semazzi HFM, Janowitz GS (1996) Response of stable stratified atmosphere to large-scale diabatic forcing with applications to wind patterns in Brazil and the Sahel. J Geo Res 101 D3:7049–7073

Wu GX (1984) The nonlinear response of the atmosphere to large-scale mechanical and thermal forcing. J Atmos Sci 41(167):2456–2476

Wu ZH (2003) A shallow CISK, deep equilibrium mechanism for the interaction between large-scale convection and large-scale circulation in the tropics. J Atmos Sci 60:377–392

Wu GX (2004) Recent progress in the study of the Qinghai-Xizang Plateau climate dynamics in China (in Chinese). Quaternary Sci 24:1–9

Wu GX, Liu HZ (1998) Vertical vorticity development owing to down-sliding at slantwise isentropic surface. Dyn Atmos Ocean 27:715–743

Wu GX, Liu YM (2000) Thermal adaptation, overshooting, dispersion, and subtropical high. Part I: Thermal adaptation and overshooting (in Chinese). Chinese J Atmos Sci 24(4):433–436

Wu GX, Liu YM (2003) Summertime quadruplet heating pattern in the subtropics and the associated atmospheric circulation. Geophys Res Lett 30:1201

Wu GX, Zhang YS (1998) Tibetan Plateau forcing and the timing of the monsoon onset over South Asia and the South China Sea. Mon Wea Rev 126:913–927

Wu GX, Liu YM, Mao JY et al (2004) Adaptation of the atmospheric circulation to thermal forcing over the Tibetan Plateau. In: Zhu X (ed) Observation, theory and modeling of atmospheric variability. World Scientific Press, London, pp 92–114

Xie P, Arkin PA (1996) Analyses of global monthly precipitation using gauge observations, satellite estimates and numerical model predictions. J Clim 9:840–858

Xie P, Arkin PA (1998) Global monthly precipitation estimates from satellite-observed outgoing longwave radiation. J Clim 11:137–164

Yanai M, Li C (1994) Mechanism of heating and the boundary layer over the Tibetan Plateau. Mon Wea Rev 122:305–323

Yanai M, Tomita T (1998) Seasonal and interannual variability of atmospheric heat sources and moisture sinks as determined from NCEP-NCAR reanalysis. J Clim 11:463–482

Yanai M, Esbensen S, Chu JH (1973) Determination of bulk propertiesof tropical cloud clusters from large-scale heat and moisture budgets. J Atmos Sci 30:611–627

Yanai M, Li C, Song Z (1992) Seasonal heating of the Tibetan Plateau and its effects of the evolution of the Asian summer monsoon. J Meteor Soc Japan 70:319–351

Yeh TC (1950) The circulation of the high troposphere over China in the winter of 1945–1946. Tellus 2(3):173–183

Yeh DC, Gao YX (1979) Meteorology of the Qinghai-Xizang (Tibet) Plateau. Science Press, Beijing, p 278

Yeh DC, Wu GX (1998) The role of the heat source of the Tibetan Plateau in the general circulation. Meteorol Atmos Phys 67:181–198

Yeh TC, Lo SW, Chu PC (1957) On the heat balance and circulation structure in troposphere over Tibetan Plateau (in Chinese). Acta Metorol Sinica 28:108–121

Yin MT (1949) A synoptic-aerologic study of the onset of the summer monsoon over India and Burma. J Meteor 6:393–400

Zhang Q, Wu GX, and Qian YF (2002) The bimodality of the 100 hPa South Asia High and its relationship to the climate anomaly over East Asia in summer. J Meteor Soc Japan 80:733–744

Zhao P, Chen LX (2001) Climate features of atmospheric heat source/sink over the Qinghai-Xizang Plateau in 35 years and its relation to rainfall in China. Sci in China Ser D 44(9):858–864

Zhu BZ (1957a) The influences of large-scale heat source or heat sink and terrain on the steady disturbance in westerlies (Part A) (in Chinese). Acta Meteorol Sinica 28(2):122–140

Zhu BZ (1957b) The influences of large-scale heat source or heat sink and terrain on the steady disturbance in westerlies (Part B) (in Chinese). Acta Meteorol Sinica 28(3):198–211